Original Article

MOLECULAR METABOLISM

Centrally circulating α-klotho inversely correlates with human obesity and modulates arcuate cell populations in mice

Taylor Landry [1,2,3,7], Peixin Li [4,7], Daniel Shookster [1,2,3], Zhiying Jiang [5], Hongli Li [5], Brenton Thomas Laing [1,2,3], Wyatt Bunner [1,2,3], Theodore Langton [1,2,3], Qingchun Tong [5], Hu Huang [1,2,3,6,*]

ABSTRACT

Objective: Our laboratory recently identified the centrally circulating α-klotho protein as a novel hypothalamic regulator of food intake and glucose metabolism in mice. The current study aimed to investigate novel molecular effectors of central α-klotho in the arcuate nucleus of the hypothalamus (ARC), while further deciphering its role regulating energy balance in both humans and mice.

Methods: Cerebrospinal fluid (CSF) was collected from 22 adults undergoing lower limb orthopedic surgeries, and correlations between body weight and α-klotho were determined using an α-klotho enzyme-linked immunosorbent assay (ELISA) kit. To investigate the effects of α-klotho on energy expenditure (EE), 2-day intracerebroventricular (ICV) treatment was performed in diet-induced obesity (DIO) mice housed in TSE Phenomaster indirect calorimetry metabolic cages. Immunohistochemical staining for cFOS and patch clamp electrophysiology were used to determine the effects of central α-klotho on proopiomelanocortin (POMC) and tyrosine hydroxylase (TH) neurons. Additional stainings were performed to determine novel roles for central α-klotho to regulate non-neuronal cell populations in the ARC. Lastly, ICV pretreatment with fibroblast growth factor receptor (FGFR) or PI3kinase inhibitors was performed to determine the intracellular signaling involved in α-klotho-mediated regulation of ARC nuclei.

Results: Obese/overweight human subjects had significantly lower CSF α-klotho concentrations compared to lean counterparts (1,044 ± 251 vs. 1616 ± 218 pmol/L, respectively). Additionally, 2 days of ICV α-klotho treatment increased EE in DIO mice. α-Klotho had no effects on TH neuron activity but elicited varied responses in POMC neurons, with 44% experiencing excitatory and 56% experiencing inhibitory effects. Inhibitor experiments identified an α-klotho → FGFR → PI3kinase signaling mechanism in the regulation of ARC POMC and NPY/AgRP neurons. Acute ICV α-klotho treatment also increased phosphorylated ERK in ARC astrocytes via FGFR signaling.

Conclusion: Our human CSF data provide the first evidence that impaired central α-klotho function may be involved in the pathophysiology of obesity. Furthermore, results in mouse models identify ARC POMC neurons and astrocytes as novel molecular effectors of central α-klotho. Overall, the current study highlights prominent roles of α-klotho → FGFR → PI3kinase signaling in the homeostatic regulation of ARC neurons and whole-body energy balance.

Keywords α-Klotho; Metabolism; Obesity; POMC neuron; Fibroblast growth factor; PI3kinase

1. INTRODUCTION

Recent evidence identifies the anti-aging protein α-klotho as a potent yet complex hormonal regulator of whole-body metabolism. α-Klotho can be secreted from the kidney [1] and act on peripheral tissues to regulate insulin sensitivity [2], promote insulin release [3,4], protect pancreatic β cells from oxidative damage [5], increase resting energy expenditure [6], and stimulate lipid oxidation [6]. Furthermore, blood α-klotho concentrations are reduced in patients with diabetes or obesity [7–11], while experimentally reversing these impairments has been shown to be therapeutic in various rodent models of metabolic disease [3–6,9].

Despite its prominent roles in peripheral metabolism, α-klotho cannot cross the blood brain barrier due to its molecular weight [12,13], resulting in a separate, relatively unexplored, pool of α-klotho secreted from the choroid plexus into the cerebrospinal fluid (CSF) [1,14]. Our laboratory recently provided the first evidence that CSF α-klotho also regulates energy balance and glucose metabolism

[1]East Carolina Diabetes and Obesity Institute, East Carolina University, Greenville, NC, USA [2]Department of Kinesiology, East Carolina University, Greenville, NC, USA [3]Human Performance Laboratory, College of Human Performance and Health, East Carolina University, Greenville, NC, USA [4]Department of Comprehensive Surgery, Medical and Health Center, Beijing Friendship Hospital, Capital Medical University, Beijing, PR China [5]Brown Foundation Institute of Molecular Medicine of McGovern Medical School, University of Texas Health Science Center at Houston, Houston, TX, USA [6]Department of Physiology, East Carolina University, Greenville, NC, USA

[7] These authors have contributed equally to this work.

*Corresponding author. Hu Huang, Department of Kinesiology and Physiology, East Carolina Diabetes and Obesity Institute, East Carolina University, 115 Heart Drive, Greenville, NC, 27834, USA. Tel.: +252 737 2879. E-mail: huangh@ecu.edu (H. Huang).

Received September 18, 2020 • Revision received November 30, 2020 • Accepted December 1, 2020 • Available online 7 December 2020

https://doi.org/10.1016/j.molmet.2020.101136

[15]. Intracerebroventricular (ICV) administration of α-klotho resulted in suppressed appetite, reduced body weight, improved insulin release, and reduced hepatic gluconeogenic gene expression in mouse models of Type I and II diabetes. We also observed that α-klotho is a novel negative regulator of neuropeptide Y/agouti-related peptide- (NPY/AgRP)-expressing neurons in the arcuate nucleus (ARC) of the hypothalamus, which are critically involved in inducing hunger [16], reducing energy expenditure [17], and regulating glucose metabolism [18,19]. Mechanistically, α-klotho acts as a scaffolding protein to promote FGFR activity and downstream PI3kinase signaling [20], a phenomenon that was found to be essential to central α-klotho-mediated regulation of energy balance and NPY/AgRP neurons [15].

The ARC contains many other cell types critical to metabolic regulation. Similar to NPY/AgRP neurons, ARC tyrosine hydroxylase-expressing (TH) neurons project to the paraventricular nucleus (PVN) to stimulate food intake [21]. Conversely, ARC proopiomelanocortin- (POMC)-expressing neurons induce satiety, increase energy expenditure, and reduce hepatic glucose output [22–24], in part via PI3kinase signaling [25]. Even non-neuronal ARC astrocytes and tanycytes are essential to nutrient sensing, hormonal transport, and neuronal health [26–28], roles recently found to be dependent on FGFR function [29,30]. Considering these diverse ARC cell types, the current study aimed to identify novel molecular effectors of the α-klotho → FGFR → PI3kinase signaling axis in the ARC, while further deciphering α-klotho's role in regulating energy balance in both humans and mice.

2. METHODS

2.1. Human cerebrospinal fluid (CSF) collection

All human protocols were approved by the medical ethics committee of Beijing Friendship Hospital, Capital Medical University (Beijing, China). After informed consent was provided, CSF was collected from 22 adults (10 males, 12 females, 18–83 years old) undergoing lower limb orthopedic surgeries at the Beijing Friendship Hospital, Beijing, China. All patients were clear of CNS infections, renal diseases, severe cardiopulmonary diseases, such as myocardial infarction or chronic obstructive pulmonary disease, and malignant tumors. Patients were chosen using systematic sampling in odd sequence on the same day each week; CSF was collected from the first, third, fifth, etc. surgery patients each day. Briefly, 1.0 ml of CSF was collected during administration of spinal block anesthesia. Patients were positioned on their sides with their backs at the edge of the operation bed, curled their shoulders and legs, and arched out their lower backs. The needle was placed past the dura mater into subarachnoid space between lumbar vertebrae, usually between L3 and L4 or L4 and L5 to minimize risk of injury to the spinal cord. All specimens were immediately flash-frozen in liquid nitrogen before storage at −80 °C. α-Klotho CSF concentrations were measured by enzyme-linked immunosorbent assay (ELISA) using a human soluble α-klotho assay kit (27,998, IBL).

2.2. Animals

C57BL/6, B6.Tg(NPY-hrGFP)1Lowl/J (NPY-GFP reporter), and Tg(Pomc1-cre)16Lowl/J (POMC-Cre) mice were cared for in accordance with the National Institutes of Health Guide for the Care and Use of Laboratory Animals, and experimental protocols were approved by the Institutional Animal Care and Use Committees of East Carolina University or University of Texas Health Science Center as appropriate. Mice were housed at 20–22 °C with a 12-h light–dark cycle.

2.3. High-fat diet-induced obesity

Five-to 6-week-old male C57BL/6 mice were given ad libitum access to a high-fat diet with a kilocalorie composition of 58%, 25%, and 17% of fat, carbohydrates, and protein, respectively, for 10 weeks (D12331; Research Diets, New Brunswick, NJ) before undergoing ICV cannulation.

2.4. ICV cannulation and treatment

ICV procedures were performed as previously described [15]. Prior to the procedure, mice were given oral analgesic meloxicam and anesthetized with an isoflurane vaporizer. Mice were placed on a stereotaxic device, and a midline incision was made on the head. A hole was drilled (1.0 mm lateral, −0.5 mm posterior, 2.5 mm deep to the bregma), and a cannula was placed into the lateral ventricle. Another hole was drilled, and a screw was placed approximately at the ipsilateral lambdoid structure to aid in supporting the cannula in the skull with 3M carboxylate dental cement. Mice recovered for 14 days before immunohistochemical experiments and 7 days before all other experiments.

ICV treatments included: 2.0 ug of α-klotho (R&D Systems) [15], 10 min of pretreatment with 25 ug of PD1703074 for FGFR inhibition (Fisher Scientific) [31], and/or 1 h of pretreatment with 10 ng of wortmannin for PI3kinase inhibition (Fisher Scientific) [32]. All ICV treatments, were administered via Hamilton syringe at a volume of 2.0 μL between 6:30 and 7:30 p.m. Validation of cannula placement was performed by post-mortem visualization of cannula path in brain slices [15].

2.5. Energy expenditure and body composition

Energy expenditure was measured using the indirect calorimetry TSE PhenoMaster metabolic cages. Diet-induced obesity (DIO) mice were placed in these cages at 16–17 weeks of age and allowed two days for acclimatization before beginning data analysis (Supplemental Fig. 1). To normalize oxygen consumption and carbon dioxide production to lean body mass, body composition was determined by Echo MRI (Echo Medical Systems, Houston, MA, USA) immediately before placement in the metabolic cages.

2.6. Food intake and body weight measurements

Food intake and body weight were measured daily. Food intake was measured by weighing food (8–9 g) and subtracting from the total food. Bedding was inspected thoroughly for residual bits of food, which were included in measurements.

2.7. Quantitative polymerase chain reaction (PCR)

To assess thermogenic gene expression, brown adipose tissue (BAT) and inguinal white adipose tissue (iWAT) was removed and flash frozen from euthanized mice after 2 days of ICV treatment with α-klotho or vehicle. RNA was extracted by Trizol (Thermo Fisher Scientific, Waltham, MA). The expression levels of specific mRNA were analyzed using quantitative real-time PCR (RT-qPCR) (Power SYBR Green PCR Master Mix; Applied Biosystems, Foster City, CA). Reactions were performed in triplicate for each sample, while 18S ribosomal RNA was used as a reference gene for normalization.

2.8. Immunohistochemistry

For immunofluorescent analysis, mice were intracardially perfused with phosphate-buffered saline (PBS) followed by 10% formalin before immunohistochemistry was performed as described previously [33]. Briefly, brains were sliced into 20-μm coronal sections using a freezing microtome (VT1000 S; Leica, Wetzlar, Germany) and

incubated overnight in antibody to phosphorylated ERK$^{thr202/tyr204}$ (1:500; Cell Signaling Technology, Danvers, MA), cFOS (1:250; Santa Cruz Biotechnology, Santa Cruz, CA), POMC (1:3,000; Phoenix Pharmaceuticals), glial fibrillary-acid protein (GFAP) (1:1,000; Millipore), tyrosine hydroxylase (TH) (1:100,000; Millipore), doublecortin (DCX) (1:800; Cell Signaling Technology), phosphorylated STAT3^{ser754} (1:3,000; Cell Signaling Technology) and/or Ki67 (1:500; Abcam), followed by incubation with Alexa-fluorophore secondary antibody for 1 h (Abcam). Stains were photographed using an optical microscope (DM6000; Leica), followed by blind analysis using ImageJ. At least 3 anatomically matched images per mouse were quantified.

2.9. Stereotaxic microinjections

To express green fluorescent protein (GFP) in POMC neurons, POMC-cre mice (7–8 weeks) were anesthetized with a mixture of ketamine (100 mg/kg) and xylazine (10 mg/kg) and placed in a stereotaxic frame. Adeno-associated viruses (AAVs) were delivered bilaterally to the ARC (200 nl/site at 30 nl/min) using the following coordinates (distances from bregma): 1.4 mm posterior, 1.6 mm lateral $\pm$ 0.2 mm, and 5.8 mm deep, with a 0.5 μl Hamilton syringe connected to a motorized stereotaxic injector (Quintessential Stereotaxic Injector; Stoelting). The injection needle was maintained in place for 5 min following injections to minimize virus spread up the needle track. The viruses used were AAV-EF1α-Flex-GFP ($> 1 \times 10^{12}$ GC/ml, UNC Vector Core) and AAV (DJ8)-Flex-mCherry ($> 1 \times 10^{12}$ GC/ml, Optogenetics and Viral Vectors Core at Baylor College of Medicine). Mice recovered for 1–2 weeks before electrophysiological recordings.

2.10. Electrophysiological recordings

Electrophysiological experiments were conducted in acutely prepared hypothalamic slices, as previously described [34,35]. Briefly, 8- to 10-week-old adult mice were deeply anesthetized with a mixture of ketamine/xylazine (intraperitoneally) and transcardially perfused with ice-cold cutting solution containing the following (in mM): 75 sucrose, 73 NaCl, 26 $NaHCO_3$, 2.5 KCl, 1.25 NaH_2PO_4, 15 glucose, 7 $MgCl_2$, and 0.5 $CaCl_2$, saturated with 95% O_2/5% CO_2. The brains were quickly removed and blocked, with the rostral face of the block glued to the specimen plate of the buffer tray then immersed in an ice-cold cutting solution. Coronal slices (280 μm) containing ARC were sectioned using a Leica VT1000S Vibratome and transferred to a holding chamber with artificial CSF (aCSF) containing the following (in mM): 123 NaCl, 26 $NaHCO_3$, 2.5 KCl, 1.25 NaH_2PO_4, 10 glucose, 1.3 $MgCl_2$, and 2.5 $CaCl_2$ and saturated with 95% O_2/5% CO_2 at 31–33 °C for 30 min, then maintained at room temperature for at least 1 h to allow for recovery before any electrophysiological recordings.

Individual slices were transferred from the holding chamber to a recording chamber, where they were submerged and continuously perfused with oxygenated aCSF at 2 ml/min. GFP-expressing POMC neurons in the ARC were first located under epifluorescence illumination, and whole-cell patch-clamp recordings were performed on 16 POMC neurons from 6 mice (3 male, 3 female) under infrared-differential interference contrast visualization at 30–32 °C on a fixed-stage, upright microscope (model BX51WI, Olympus) equipped with a water-immersion 40 × objective. Pipettes with a resistance of 3–5 MΩ were pulled from borosilicate glass (outer diameter, 1.5 mm; inner diameter, 1.1 mm; Sutter Instruments) using a horizontal puller (P-97, Sutter) and filled with an internal patch solution containing the following (in mM): 142 K-gluconate, 10 HEPES, 1 EGTA, 2.5 $MgCl_2$, 4 Mg-ATP, 0.3 Na-GTP, and 10 Na_2-phosphocreatine, adjusted to pH 7.25–7.35, osmolality 295–305 with KOH. After "breaking into" cells, at least 5 min was given for baseline to be established before obtaining baseline measurements for another 5–9 min. α-Klotho was then administered at 3.65 mM in aCSF. The liquid junction potential was not corrected, and series resistance (Rs) was bridge balanced.

2.11. Statistical analysis

Pearson's correlation coefficients were used to determine associations between CSF α-klotho concentrations and other variables. Unpaired t-tests or one-way analysis of variance (ANOVA) with Tukey's correction for multiple comparisons were used to determine differences between or among groups, respectively, in CSF α-klotho, oxygen consumption, carbon dioxide production, locomotor activity, gene expression, food intake, body weight, or proteins of interest detected by immunofluorescence. To compare pre-post within-group changes over the course of 2-day experiments, paired t-tests were performed. Unpaired or paired *t*-tests were used for between or within-neuron patch clamp electrophysiology experiments, respectively. All analyses were performed using GraphPad Prism statistics software, and $p < 0.05$ was considered statistically significant.

2.12. Data availability statement

The data sets generated during the current study are available from the corresponding author on reasonable request.

3. RESULTS

3.1. Human CSF α-klotho concentrations are reduced in overweight and obese adults

CSF was collected from 22 adults (10 males, 12 females) with an average age and body mass index (BMI) of 52.3 $\pm$ 17.1 and 25.7 $\pm$ 3.6, respectively (Supplemental Table 1). CSF α-klotho concentrations exhibited a strong inverse correlation with body weight and BMI ($R = -0.6823$ and -0.7822 respectively) (Figure 1A–B). There were no correlations between CSF α-klotho concentrations and fasting blood glucose, cholesterol, or triglycerides (Figure 1D–F). Subjects were then stratified into lean (BMI<25) and overweight/obese (BMI>25) categories (mean BMI's were 22.8 $\pm$ 1.7 and 28.6 $\pm$ 2.4, respectively). Although there were no significant differences in age, height, fasting blood glucose, blood triglycerides, total cholesterol, or LDL levels between the groups (Supplemental Table 1), overweight/obese subjects had significantly lower CSF α-klotho concentrations and serum high-density lipoprotein (HDL) levels compared to lean counterparts (1,044 $\pm$ 251 vs. 1,616 $\pm$ 218 pmol/L and 1.2 $\pm$ 0.2 vs. 1.0 $\pm$ 0.2 mmol/L, respectively) (Figure 1C and Supplemental Table 1). To our knowledge, this is the first study to illustrate a strong negative correlation between CSF α-klotho and body weight in human subjects, suggesting the potential involvement of central α-klotho in the development of obesity.

3.2. Two days of ICV α-klotho treatment increases energy expenditure in DIO mice

To further investigate the role of central α-klotho in energy balance regulation, 2 days of ICV α-klotho treatment was performed in male DIO mice. Consistent with previous results, 2 days of ICV α-klotho treatment significantly decreased daily food intake (20.3%) and resulted in modest reductions in body weight (1.5%) compared to vehicle-treated controls (Supplemental Fig. 2). ICV α-klotho treatment also significantly increased average daily oxygen consumption (10.9%) and carbon dioxide production (11.2%), with no effects on locomotor activity (Figure 2A–F). These data suggest a novel ability of central α-klotho to improve energy balance by increasing daily energy expenditure.

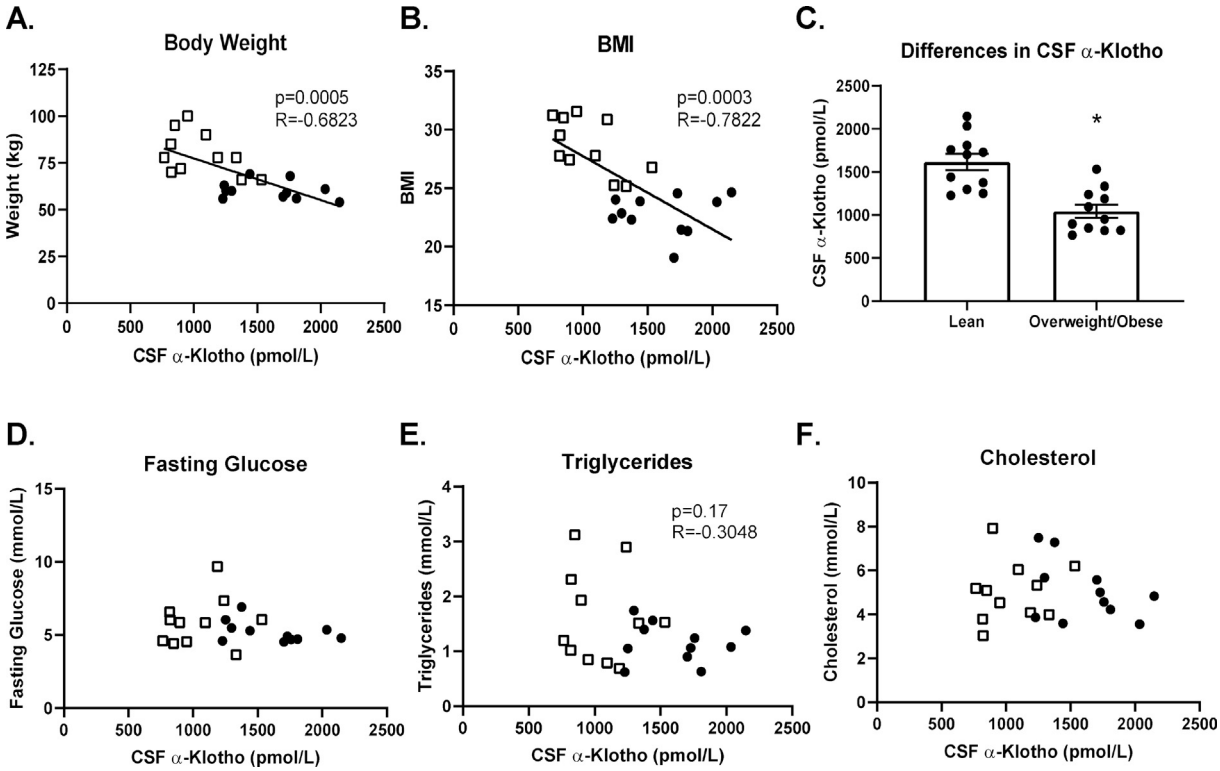

Figure 1: Cerebrospinal fluid α-klotho concentrations are reduced in overweight and obese adults. CSF α-klotho concentrations are inversely correlated with (A) Body weight and (B) BMI (n = 22). (C) Comparison of CSF α-klotho concentrations when subjects are stratified into lean vs. overweight/obese categories based on BMI. (n = 11/group). CSF α-klotho concentrations are not correlated with (D) fasting blood glucose, (E) triglycerides, or (F) cholesterol. ● represents lean; □ represents overweight or obese. Data represented as mean ± SEM. * indicates $p < 0.05$ vs. lean subjects.

UCP1 gene expression also tended to be elevated in BAT and iWAT of α-klotho-treated mice (1.4-fold; p = 0.07 and 6.4-fold; p = 0.11, respectively), suggesting potentially increased thermogenesis and browning of white adipose tissue (Figure 2G—H). There were also trends toward increased NRF1 gene expression in the BAT of α-klotho-treated mice (1.3-fold; p = 0.09), while there were no differences in PRDM16, CIDEA, PGC1α, or PPARγ gene expression in either BAT or iWAT.

3.3. Central α-klotho has no obvious effects on TH neuron activity in fasted mice

Previous reports identify direct, inhibitory action of central α-klotho on ARC NPY/AgRP neurons [15]; thus, we aimed to investigate the possibility of additional neuronal targets of central α-klotho in the hypothalamus. For example, TH neurons elicit orexigenic effects in the ARC and regulate thermogenesis in the PVN [21,36]. However, immunofluorescent staining revealed acute ICV α-klotho treatment had no obvious effects on cFOS colocalization with TH neurons in the hypothalami of fasted male or female mice (Figure 3).

3.4. Central α-klotho regulates ARC POMC neuron activity in fasted mice

POMC neurons are another ARC neuron population involved in reducing hunger and increasing energy expenditure [22—24]. We performed patch clamp electrophysiology experiments and 7 out of 16 POMC neurons analyzed exhibited increased firing rate and membrane potential when treated with α-klotho (0.47 ± 0.13 vs. 1.40 ± 0.28 Hz and −50.52 ± 1.02 vs. −47.57 ± 1.17 mV, respectively) (Figure 4A—C). Interestingly, all POMC neurons recorded responded to α-klotho, with 9 out of 16 POMC neurons exhibiting decreased firing rate and membrane potential (0.30 ± 0.09 vs. 0.08 ± 0.06 Hz and −47.33 ± 0.73 vs. −52.10 ± 1.76 mV, respectively) (Supplemental Figs. 3A—C). While these data identify POMC neurons as novel neuronal effectors of central α-klotho function, they also highlight the heterogeneity of the POMC-expressing neuron population [37]. For example, POMC neurons stimulated by α-klotho had significantly lower baseline membrane potentials compared to those antagonized by α-klotho, while there were no differences in baseline firing rate (Supplemental Figs. 3D—E).

To further investigate the complex effects of central α-klotho on ARC POMC neuron activity, we performed immunofluorescent staining for cFOS. While acute ICV α-klotho treatment had no effects on ARC POMC neuron activity in fed mice (Supplemental Fig. 4), cFOS colocalization with ARC POMC neurons was significantly elevated in response to acute ICV α-klotho treatment in both fasted male (1.9-fold) and female (1.7-fold) mice (Figure 4D—J). These data highlight potent excitatory effects of α-klotho on ARC POMC neurons in the fasted status, despite the heterogenous response of POMC neurons observed in electrophysiology experiments.

3.5. Central α-klotho increases ARC POMC neuron activity, at least in part, via FGFR's

Previous studies demonstrate α-klotho's role as a scaffolding protein to facilitate FGF23-FGFR binding and downstream signaling, a phenomenon that was found to be critical to α-klotho-mediated NPY/AgRP neuron inhibition [15,20,38]. To investigate the importance of FGFR's

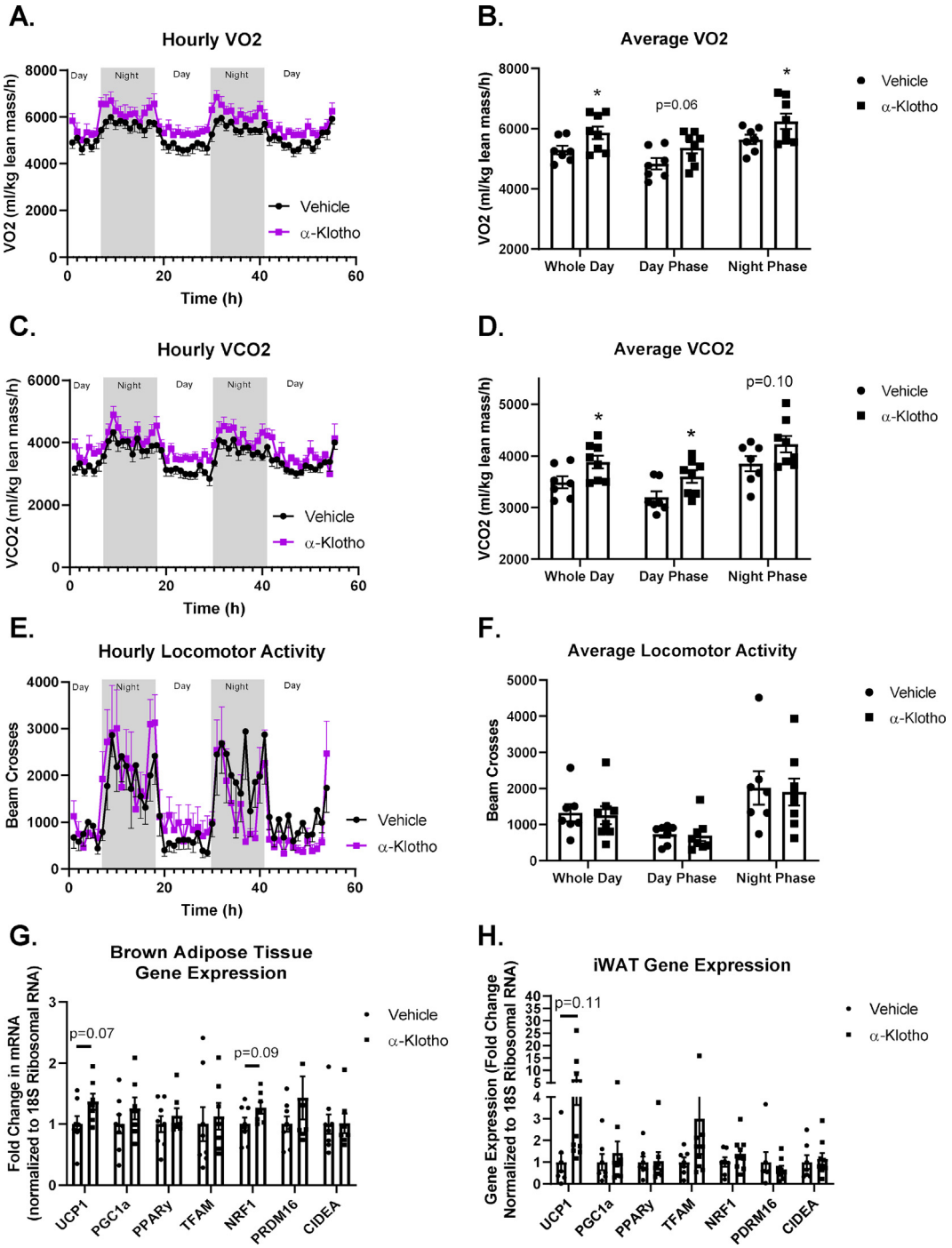

Figure 2: Two days of ICV α-klotho treatment increases energy expenditure in DIO mice. (A–B) Oxygen consumption, (C–D) carbon dioxide production, and (E–F) locomotor activity in 16- to 17-week-old male DIO mice after 2 days ICV α-klotho (2.0 ug) or vehicle (2.0 uL) injections (n = 7–8/group). (G) BAT gene expression and (H) iWAT gene expression (n = 7–9/group). Data represented as mean ± SEM. * indicates $p < 0.05$ vs. vehicle controls.

to α-klotho-mediated POMC activation, ICV pretreatment with the FGFR inhibitor PD173074 was performed. When FGFR activity was inhibited, α-klotho no longer significantly increased POMC neuron activity (1.4-fold increase under FGFR blockade, $p = 0.13$; vs. 2.1-fold increase with vehicle-treated controls, $p < 0.05$) (Figure 5). The blunted effects of α-klotho in response to FGFR inhibition may indicate central α-klotho regulates POMC neurons, at least in part, via FGFR activity (Figure 5).

3.6. α-Klotho/PI3kinase signaling regulates ARC POMC and NPY/AgRP neuron activity

PI3kinase is a prominent signaling mechanism in the regulation of energy balance, ARC neuron activity, and α-klotho-mediated down-regulation of AgRP gene expression [15,25]. When central PI3kinase signaling was impaired using ICV wortmannin treatment, α-klotho no longer significantly increased POMC neuron activity compared to PI3kinase inhibition alone (Figure 6). Past experiments from our lab

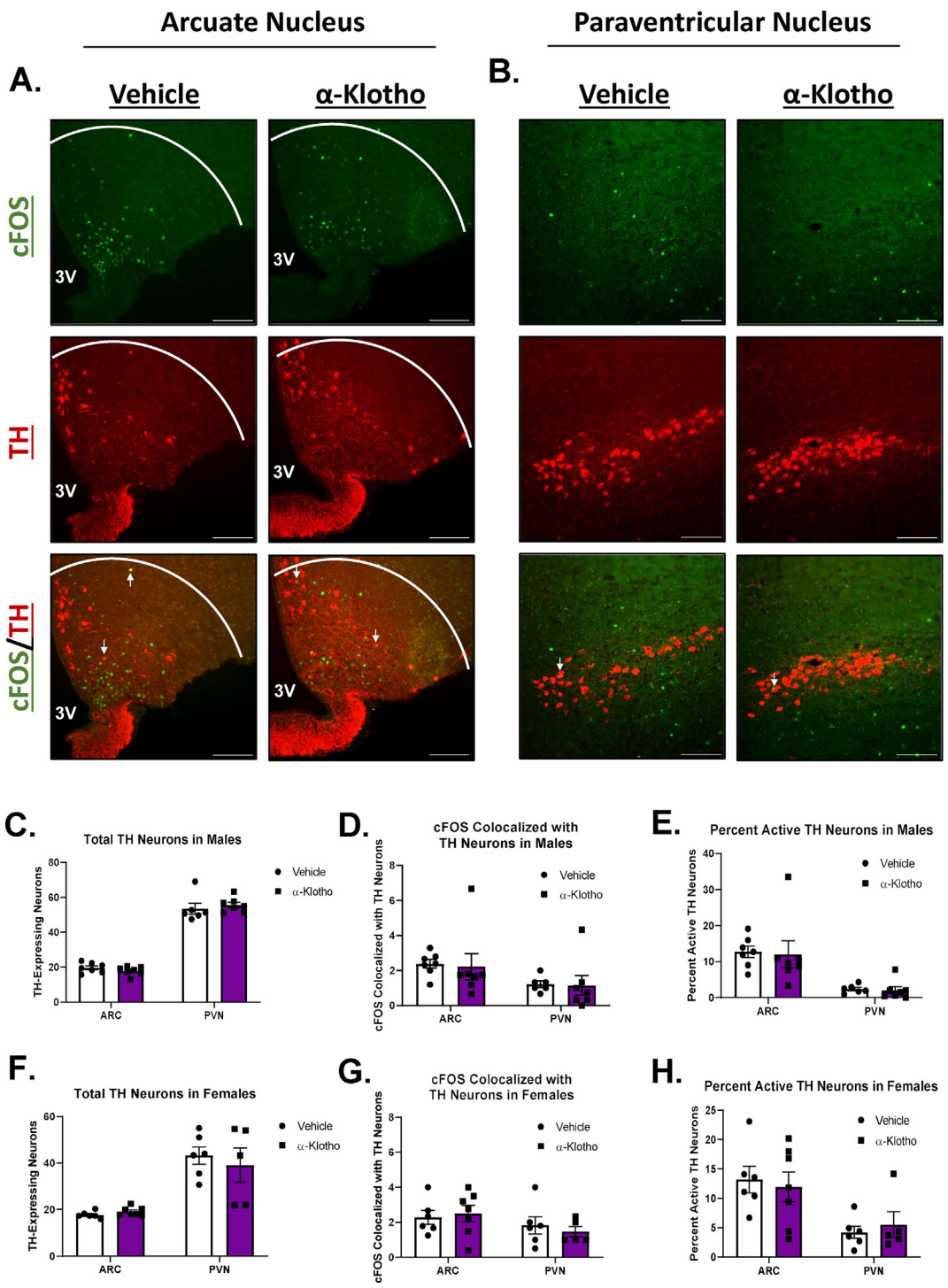

Figure 3: Acute ICV α-klotho treatment has no effects on TH-expressing neuron activity in the ARC or PVN. Representative images of cFOS (green) colocalized with TH-expressing neurons (red) in the (A) ARC and (B) PVN of mice acutely treated with ICV vehicle (2.0 uL) or α-klotho (2.0 ug) before an overnight fast. (C) Total TH-expressing neurons, (D) cFOS colocalization, and (E) proportion of active TH-expressing neurons in male mice (n = 6–7/group). (F) Total TH-expressing neurons, (G) cFOS colocalization, and (H) proportion of active TH-expressing neurons in female mice (n = 5–7/group). 3V = Third ventricle; scale bar = 50 um. Data represented as mean ± SEM. * indicates $p < 0.05$ vs. vehicle controls.

also indicate α-klotho downregulates AgRP gene expression via PI3kinase signaling [15]. Consistent with previous reports, in the current study, acute ICV α-klotho treatment significantly reduced NPY/AgRP neuron activity (46%) (Figure 7). Furthermore, PI3kinase inhibition attenuated this α-klotho-mediated suppression of NPY/AgRP neuron activity (Figure 7). Overall, these data suggest PI3kinase signaling is critical to α-klotho-mediated regulation of both NPY/AgRP and POMC neurons.

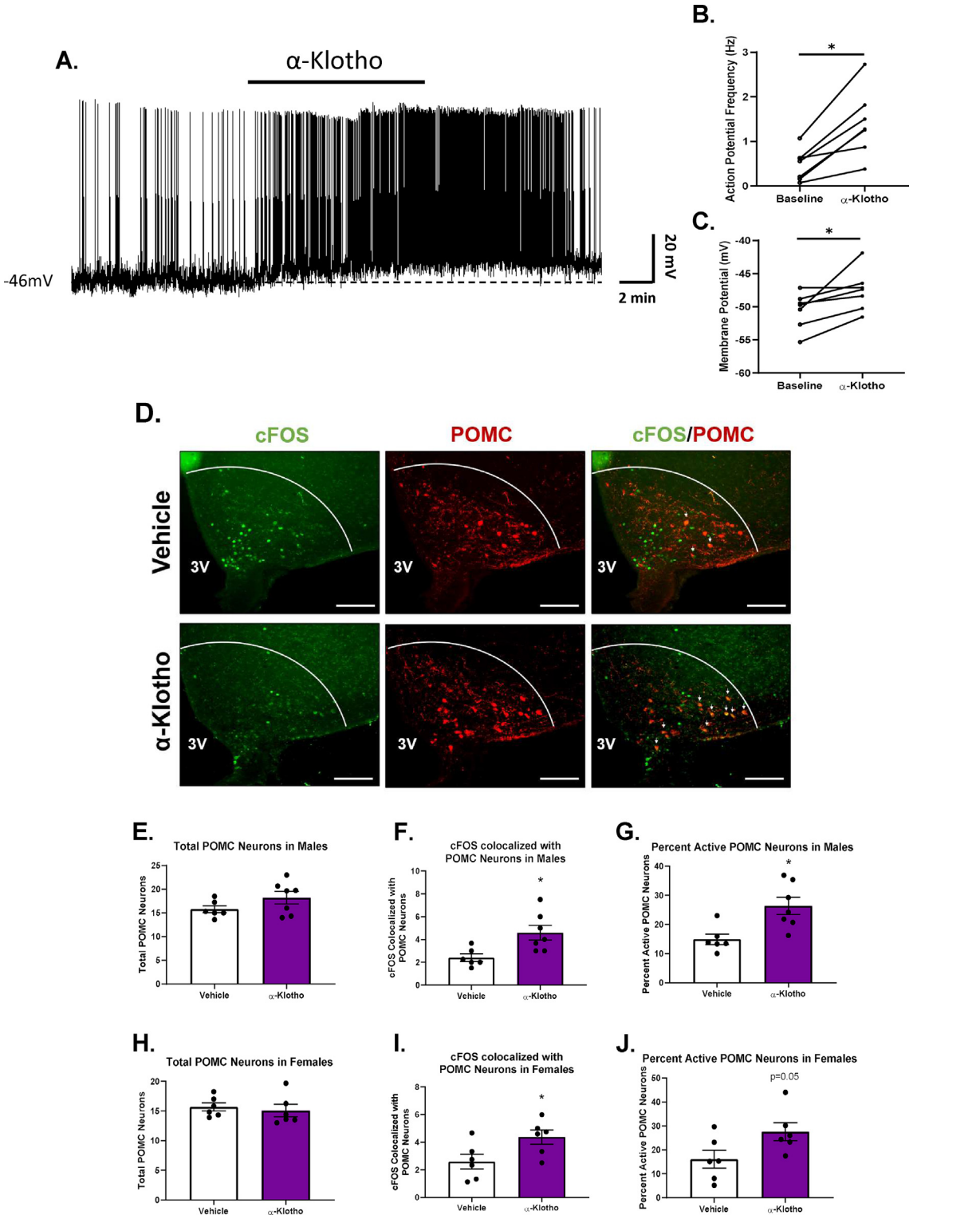

Figure 4: Acute ICV α-klotho treatment increases ARC POMC neuron activity in fasted mice. (A) Representative whole cell patch clamp recording, (B) action potential frequency, and (C) membrane potential of a POMC neuron stimulated by α-klotho treatment (n = 7 neurons). (D) Representative images of cFOS (green) colocalized with POMC (red) in the ARC of healthy, male mice acutely treated with ICV α-klotho (2.0 ug) or vehicle (2.0 uL) before an overnight fast. (E) Total POMC neurons, (F) cFOS colocalization, (G) and proportion of active POMC neurons in male mice (n = 6–7/group). (H) Total POMC neurons, (I) cFOS colocalization, and (J) proportion of active POMC neurons in female mice (n = 6/group). 3V = Third ventricle; scale bar = 50 um. Data represented as mean ± SEM. * indicates $p < 0.05$ vs. vehicle controls.

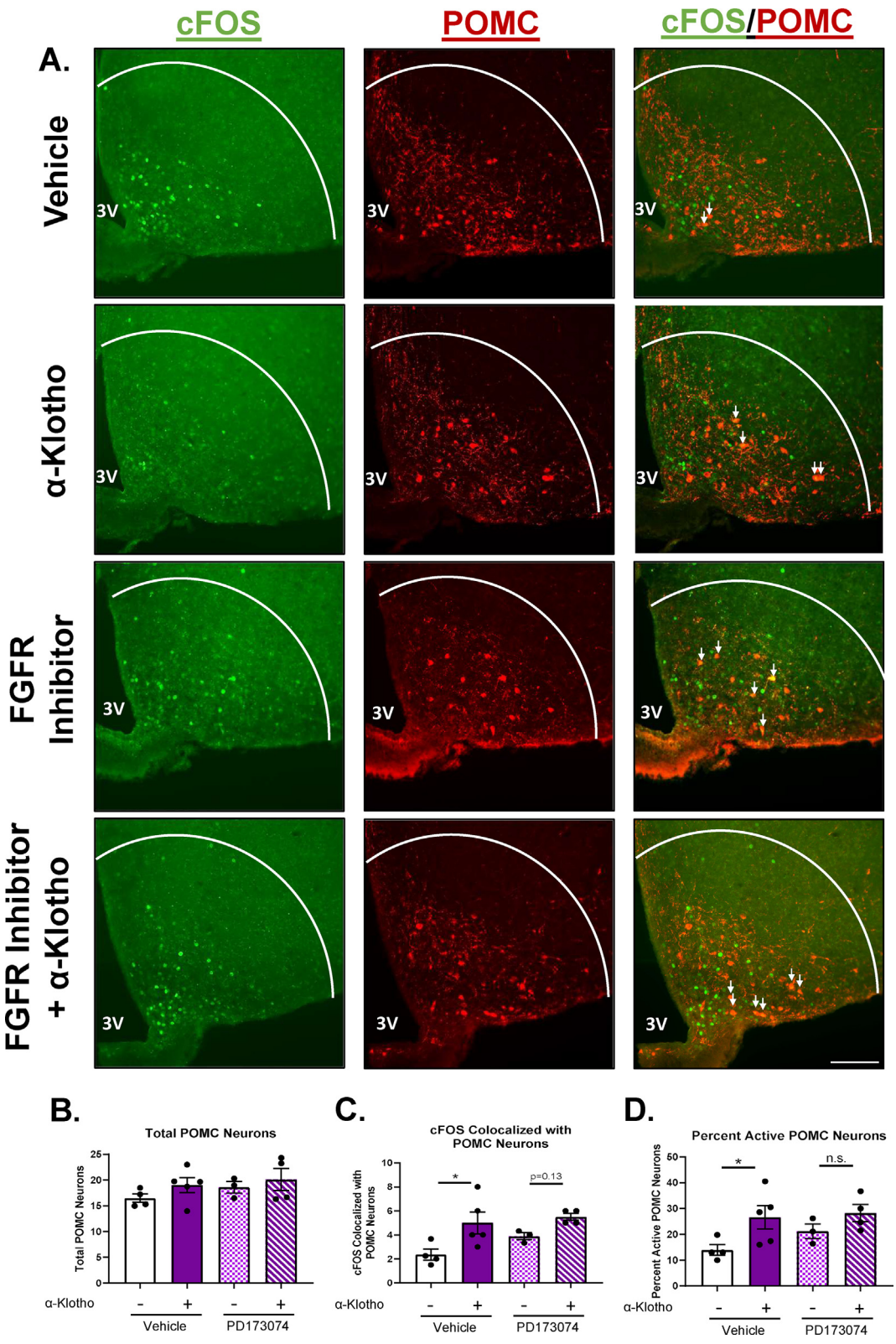

Figure 5: Central α-klotho increases ARC POMC neuron activity, at least in part, via FGFR's. (A) Representative images of cFOS (green) colocalized with POMC (red) in the ARC of healthy, male mice acutely treated with vehicle (2.0 uL), α-klotho (2.0 ug), FGFR inhibitor alone (25 ug), or FGFR inhibitor 10 min before α-klotho before an overnight fast. (B) Total POMC neurons, (C) cFOS colocalization, and (D) proportion of active POMC neurons (n = 3–5/group). 3V = Third ventricle; scale bar = 50 um. Data represented as mean ± SEM. n.s = not significant; * indicates $p < 0.05$.

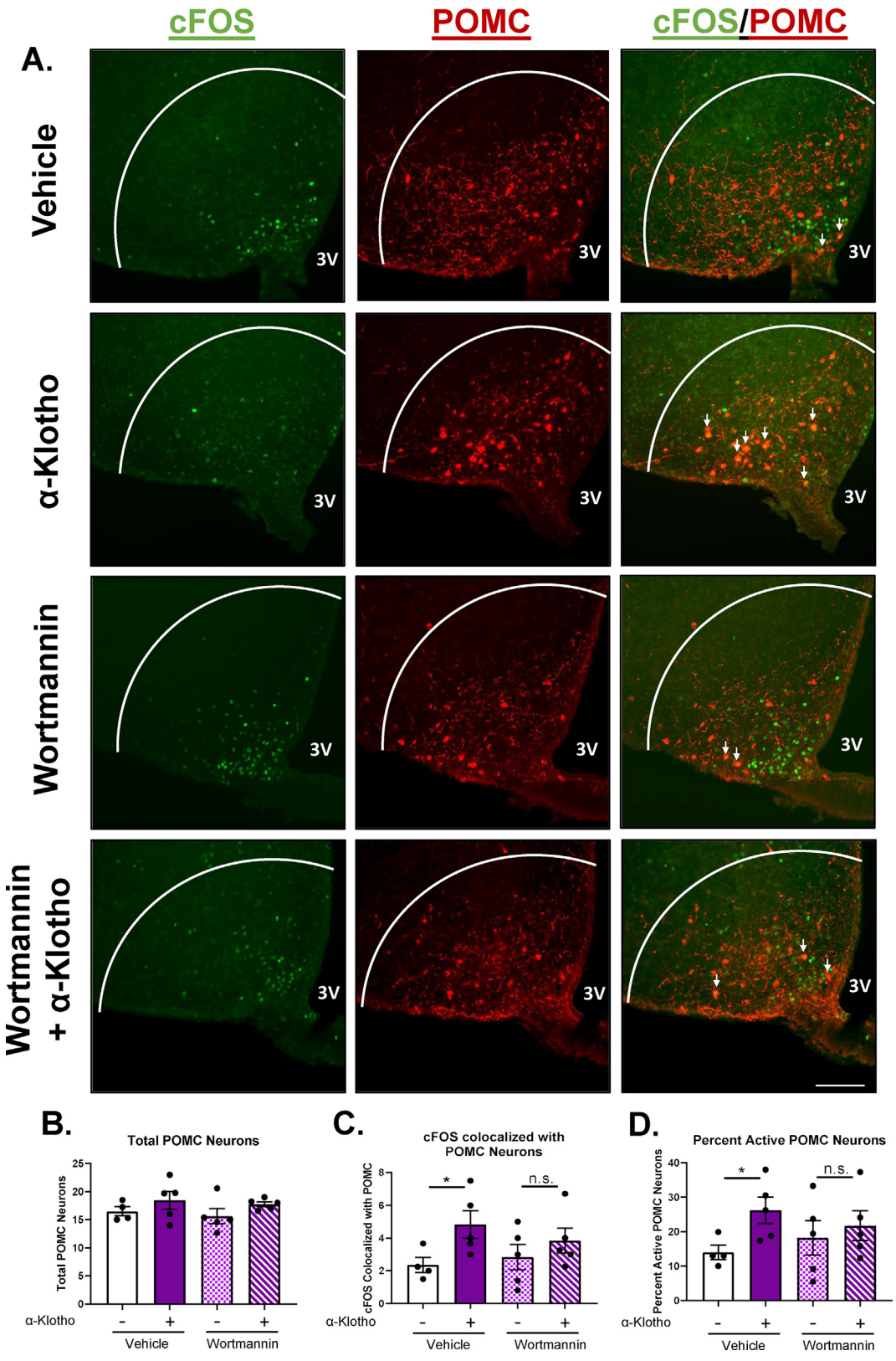

Figure 6: PI3kinase inhibition blunts α-klotho-mediated ARC POMC neuron activation. (A) Representative images of cFOS (green) colocalized with POMC (red) in the ARC of healthy, male mice acutely treated with vehicle (2.0 uL), α-klotho (2.0 ug), wortmannin alone (10 ng), or wortmannin 1 h before α-klotho before an overnight fast. (B) Total POMC neurons, (C) cFOS colocalization, and (D) proportion of active POMC neurons (n = 4–5/group). 3V = Third ventricle; scale bar = 50 um. Data represented as mean ± SEM. n.s = not significant; * indicates $p < 0.05$.

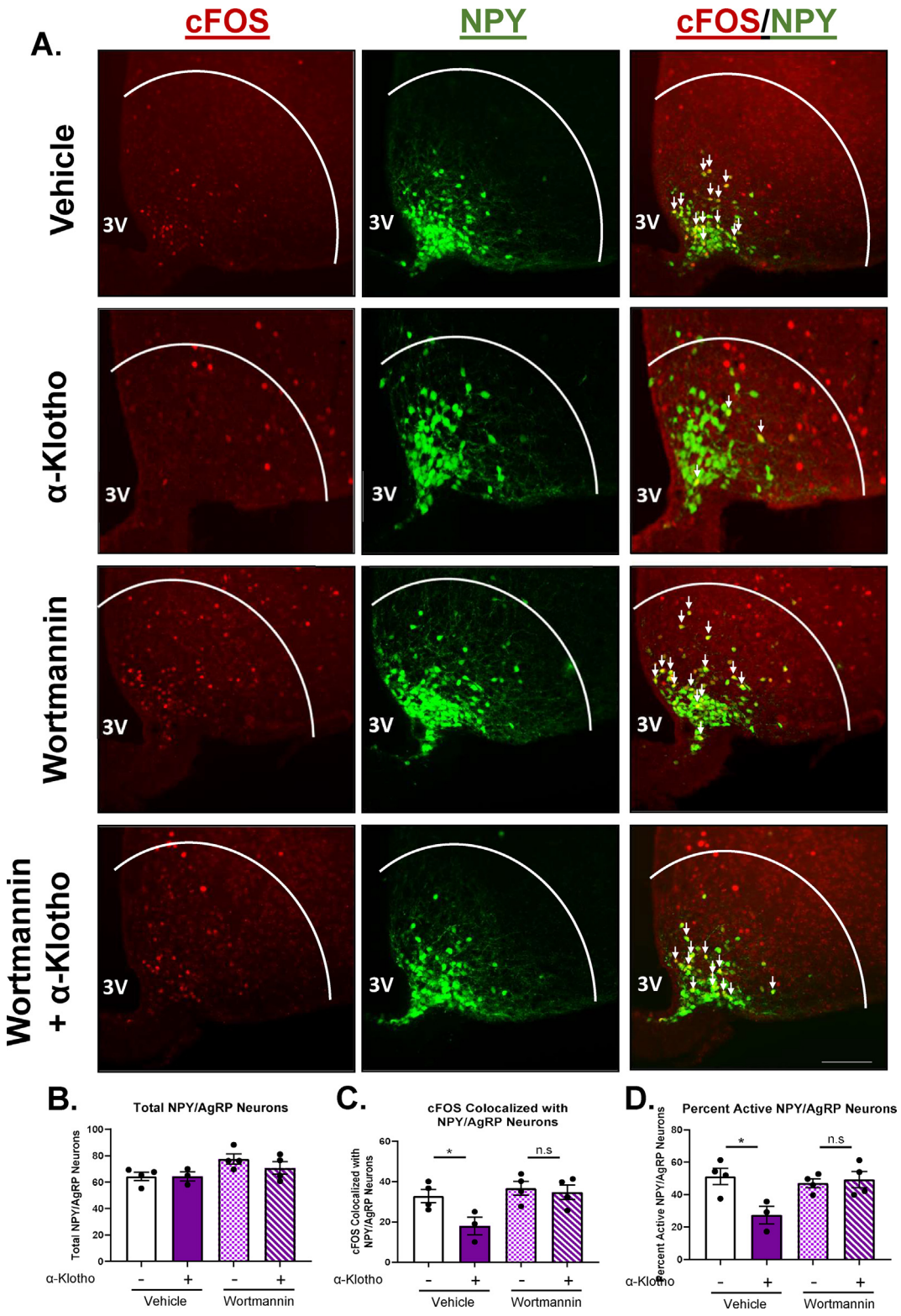

Figure 7: PI3kinase inhibition abolishes α-klotho-mediated ARC NPY/AgRP neuron inhibition. (A) Representative images of cFOS (red) colocalized with NPY/AgRP (green) in the ARC of healthy, male mice acutely treated with vehicle (2.0 uL), α-klotho (2.0 ug), wortmannin alone (10 ng), or wortmannin 1 h before α-klotho before an overnight fast. (B) Total NPY/AgRP neurons, (C) cFOS colocalization, and (D) proportion of active NPY/AgRP neurons (n = 3–4/group). 3V = Third ventricle; scale bar = 50 um. Data represented as mean ± SEM. n.s = not significant; * indicates $p < 0.05$.

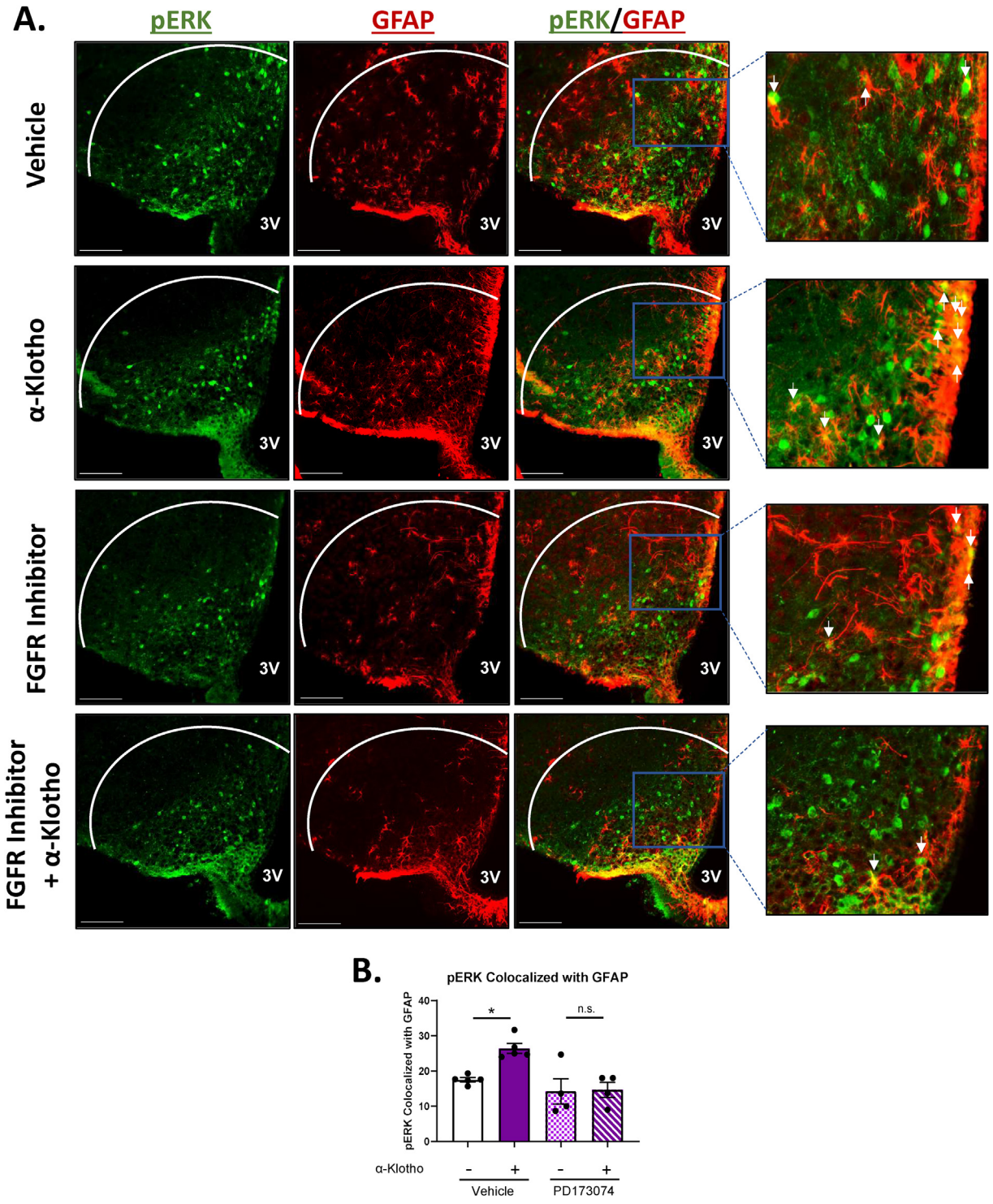

Figure 8: Acute ICV α-klotho treatment stimulates pERK$^{thr202/tyr204}$ in astrocytes. (A) Representative images of pERK$^{thr202/tyr204}$ (green) colocalized with GFAP (red) in the ARC of healthy, male mice acutely treated with vehicle (2.0 uL), ICV α-klotho (2.0ug), FGFR inhibitor alone (25 ug), or FGFR inhibitor 10 min before α-klotho (2.0 ug) before an overnight fast. (B) pERK$^{thr202/tyr204}$ colocalized with GFAP. 3V = Third ventricle; scale bar = 50 um. Data represented as mean ± SEM. n.s = not significant; * indicates $p < 0.05$.

3.7. ICV α-klotho treatment increases phosphorylated ERK$^{thr202/tyr204}$-in ARC astrocytes

We next aimed to determine whether central α-klotho was involved in the regulation of ARC astrocytes, cells involved in nutrient sensing, hormonal transport, and neuronal health [26]. ERK signaling is a key regulatory mechanism in astrocyte function and has also been identified as a downstream signaling mechanism of α-klotho in the ARC [15,27,28,39]. There were distinct differences in the localization of

phosphorylated ERK$^{thr202/tyr204}$ in the ARC between the two groups. α-Klotho-treated mice exhibited 1.4-fold higher pERK$^{thr202/tyr204}$ in cells expressing the astrocytic marker GFAP (Figure 8), with qualitatively higher pERK$^{thr202/tyr204}$ concentration in the tanycytic region bordering the third ventricle. Mechanistically, pretreatment with the FGFR inhibitor PD173074 completely abolished this phenomenon (Figure 8).
Overall, these data may indicate a novel role for central α-klotho/FGFR signaling to regulate astrocyte function in the ARC, suggesting involvement in supporting other nutrient-sensing and hormonal functions. For example, leptin sensitivity and transport are closely connected to astrocyte function [27,28]. Supporting the hypothesis that α-klotho facilitates hormonal transport and sensitivity, acute ICV α-klotho treatment in fasted mice significantly increased phosphorylated STAT3 2.1-fold in NPY/AgRP neurons, which is an inhibitory signaling mechanism in these neurons and a critical downstream mediator of leptin (Supplemental Fig. 5).
Furthermore, longer duration (12-days) α-klotho treatment increased Ki67 expression 3.0-fold in the ARC (Supplemental Fig. 6), which is an indication of increased proliferating cells. This increase in active progenitor cells is likely non-neuronal, demonstrated by no effects of long-term α-klotho treatment on number of total POMC, NPY/AgRP, and DCX- (a marker of neurogenesis) expressing cells in the ARC (Supplemental Fig. 7). However, the anatomical distribution of Ki67 expression in the ARC suggests that the proliferating cells may be astrocytes or tanycytes, which would indicate that α-klotho not only regulates the function of mature astrocytes, but may also be involved in the generation of new astrocytes.

4. DISCUSSION

A recent study from our laboratory provided promising evidence that central α-klotho may be a critical regulator of hypothalamic neurons and metabolism [15]. Aiming to more comprehensively decipher central α-klotho's metabolic role, the current study identified diverse novel functions of central α-klotho in the regulation of energy balance and ARC cell populations. Our data indicates central α-klotho increases energy expenditure, modulates NPY/AgRP and POMC neuron activity via FGFR → PI3kinase signaling, and regulates astrocytes via FGFR → ERK signaling. Furthermore, to our knowledge, we provide the first evidence that CSF α-klotho concentrations and body weight exhibit a strong inverse correlation in humans, potentially implicating central α-klotho in the pathology of obesity.
Previous reports have indicated that blood α-klotho concentrations are impaired in humans with diabetes [7,8]. However, there is no correlation between peripheral and central α-klotho concentrations, and regulation of circulating CSF α-klotho levels is poorly understood [40]. The few studies examining CSF α-klotho concentrations have determined no diurnal variations [41], decreased levels in females [40,41], an inverse correlation with age [41], and a positive correlation with FGF23 [40]. Additionally, human CSF α-klotho concentrations are reduced in some neurological disorders, such as Alzheimer's disease [41] and multiple sclerosis [42]. We observed that CSF α-klotho levels exhibit a strong, inverse correlation with body weight and BMI. These data may suggest the involvement of central α-klotho in the pathology of obesity and could possibly identify CSF α-klotho levels as a novel preclinical marker in body weight disorders. Considering previous data showing ICV α-klotho treatment improves hepatic lipid accumulation and central α-klotho inhibition rapidly impairs glucose clearance [15], we also hypothesized that CSF α-klotho may inversely correlate with blood glucose, TG's, or cholesterol. Surprisingly, no such correlations were observed, nor were there significant differences in these variables between lean and overweight/obese subjects. Notably, blood glucose, TG's, and cholesterol often exhibit a weak relationship with BMI [43–45], and a limitation of the current study is a small sample size. Future studies utilizing a larger sample size may reveal additional correlations between CSF α-klotho concentrations and blood glucose or lipids.
Consistent with previous reports, ICV α-klotho treatment suppressed food intake and resulted in modest body weight reductions in DIO mice [15]. Indirect calorimetry also determined that ICV α-klotho treatment increases resting energy expenditure independent of locomotor activity. Gene expression analysis revealed that increased thermogenesis in BAT and browning of iWAT may be the mechanism underlying increased energy expenditure. While the mechanism for α-klotho-mediated increases in energy expenditure remains unclear, these data highlight a potent role for central α-klotho to improve energy balance by regulating both caloric consumption and utilization.
The observed ICV α-klotho phenotype may be a result of its diverse functions regulating the intricate neurocircuitry in ARC cell populations. For example, α-klotho is an antagonist of ARC NPY/AgRP neurons [15], which, when activated, stimulate food intake, increase circulating glucose levels, decrease energy expenditure, and result in weight gain [16–19]. Here, we identify α-klotho as a novel modulator of ARC POMC neurons, which have opposite metabolic effects compared to NPY/AgRP neurons [24,46]. α-Klotho elicited varied effects on POMC neurons during electrophysiological experiments, with 44% experiencing excitatory and 56% experiencing inhibitory effects. These findings highlight the heterogeneity of the POMC neuron population, with 72% being "canonical", expressing high levels of POMC and very low levels of AgRP, and 28% expressing low levels of POMC and high levels of AgRP [37]. α-Klotho decreases AgRP gene expression and inhibits AgRP-expressing neuron activity [15], which may suggest that α-klotho inhibits the POMC neurons expressing high levels of AgRP. Additionally, POMC neurons have variable receptor and neurotransmitter expression, which likely also alters their response to α-klotho [37,47].
It is also possible α-klotho regulates POMC neurons indirectly via presynaptic inputs. For example, α-klotho's previously documented direct inhibitory role in NPY/AgRP neurons [15] may indirectly stimulate POMC activity via relieved NPY/AgRP-mediated GABAergic inputs. Interestingly, NPY/AgRP → POMC connectivity is complex, highlighted by differences in the effects of spontaneous vs. stimulated NPY/AgRP neuron activity. POMC neurons exhibit no change in inhibitory postsynaptic currents (IPSC's) when NPY/AgRP neuron activity or neurotransmitter release is disrupted [48,49]; however, optogenetic stimulation of NPY/AgRP neurons consistently inhibits POMC neurons via direct GABAergic inputs [48,50]. Notably, the current study determined that α-klotho regulates NPY/AgRP and POMC neurons via FGFR's, which are expressed in both populations [51]. As a result, α-klotho can likely elicit direct, postsynaptic regulation of both of these neurons via its role as a scaffolding protein in FGFR's.
Orexigenic ARC TH neurons are also intricately involved in NPY/AgRP and POMC neurocircuitry. For example, TH and NPY/AgRP neurons exhibit a bidirectional synaptic mechanism during which TH neurons stimulate food intake via direct excitatory dopamine action on NPY/AgRP neurons, and NPY/AgRP neurons regulate thermogenesis via Y1 receptors on TH neurons [21,36,52]. Furthermore, both dopamine and GABA released from TH neurons exhibit direct inhibitory action on POMC neurons. Similar to POMC neurons, TH neurons are also a heterogenous neuron population. TH is the rate-limiting enzyme in dopamine and catecholamine synthesis [53], both of which have varied effects on metabolism. For example, dopamine stimulates food intake [52], and catecholamines induce satiety [54,55]. In the current study,

ICV α-klotho had no significant effects on ARC or PVN TH neuron activity, suggesting TH neurons may not be involved in α-klotho's hypothalamic function. However, one α-klotho-treated mouse appeared to be a statistical outlier (greater than two standard deviations different from the mean). Removal of this animal reveals trends toward α-klotho-mediated TH neuron suppression in males only, highlighting the need for further research into this phenomenon. Overall, while the current study does not identify a specific role of α-klotho to regulate hypothalamic TH neurons, future studies using electrophysiology on single TH neurons would help clarify these complicated findings among different TH subpopulations.

We also aimed to determine whether α-klotho had additional functions in the ARC independent of neuronal activity. In hippocampal cells, α-klotho has been described as a regulator of neurogenesis and astrocyte metabolism [39,56]. While there were no effects of α-klotho on ARC neurogenesis in DIO mice, we did observe an ability of α-klotho to regulate astrocyte function. ARC astrocytes are critically involved in hormonal transport, nutrient sensing, and neuronal maintenance [27], and α-klotho treatment increased phosphorylated ERK specifically in this cell type. ERK signaling in astrocytes is essential to leptin transport through the blood brain barrier [28], suggesting a novel role for central α-klotho to regulate hormonal transport. This hypothesis was supported by increased phosphorylated STAT3, a key downstream mediator of leptin, in NPY/AgRP neurons in response to α-klotho treatment. Considering the diverse functions of central α-klotho in the ARC, deciphering the molecular mechanisms involved is essential to understanding the complex questions surrounding homeostatic and disordered regulation of metabolism.

α-Klotho has a well-documented role as a scaffolding protein in the FGF23 → FGFR complex [20], and experimental FGFR activation has recently been shown to elicit therapeutic effects in metabolic disease models [51,57,58]. We determined that α-klotho regulates astrocytes via an FGFR → ERK mechanism, similar to the mechanism underlying sustained diabetes remission in response to acute FGF1 microinjection [29]. Interestingly, α-klotho only significantly increased POMC neuron activity when FGFR's were functional. This suggests that α-klotho may regulate POMC neurons via FGFR's, but concurrent receptors are likely involved. Notably, the specific receptor of α-klotho is currently not known, but one potential mechanism could be through transient receptor potential vanilloid-like (TRPV) channels. TRPV channels increase POMC neuron activity to reduce food intake [59], and α-klotho has a well-documented role to hydrolyze these receptor like-channels in renal tubules and pancreatic β cells to increase their membrane localization [3,4,60].

PI3Kinase is another potent regulator of ARC neuron populations and a downstream effector of α-klotho [15,25]. While it has previously been shown that PI3kinase is essential to α-klotho-mediated AgRP mRNA downregulation, it was unclear whether PI3kinase was equally important to α-klotho-mediated NPY/AgRP neuron inhibition [15]. The current study showed PI3kinase inhibition completely abolished α-klotho-mediated NPY/AgRP neuron inhibition and POMC activation. These data indicate a prominent α-klotho → FGFR → PI3kinase signaling axis involved in the regulation of ARC neuron populations.

5. CONCLUSIONS

To summarize, this study identified diverse novel functions of α-klotho in the ARC via various molecular mechanisms. Experiments revealed that α-klotho regulates astrocytes via FGFR → ERK signaling, as well as NPY/AgRP neurons and POMC neurons via FGFR → PI3kinase signaling. Furthermore, CSF α-klotho's prominent role in energy balance was demonstrated by strong inverse correlations with body weight and an ability to increase energy expenditure. Further investigation on these novel molecular mechanisms could be integral to deciphering the complex physiology underlying homeostatic and disordered regulation of metabolism.

AUTHOR CONTRIBUTIONS

T.L. conceptualization, methodology, validation, formal analysis, investigation, writing — original draft, writing — review and editing, and visualization; P.L. conceptualization and investigation; D.S. investigation, writing — review and editing; Z.J. investigation; H.L. investigation; B.T.L. conceptualization; W.B. conceptualization, formal analysis; Q.T. supervision, project administration, funding acquisition; H.H. conceptualization, writing — review and editing, supervision, project administration, funding acquisition.

GUARANTOR STATEMENT

Dr. Hu Huang is the guarantor of this work, and, as such, has full access to all the data in the study and takes responsibility for its integrity and the accuracy of the analysis.

FUNDING

The funding for this project was provided by East Carolina University start-up funds and the NIH (DK121215) to HH. Additional funding was provided by NIH RO1DK114279, R21NS108091, RO1DK120858, and DOD W81XWH-19-1-0429 to QT.

ACKNOWLEDGMENTS

We would like to thank Dr. Erzsebet Szatmari (College of Allied Health Sciences, East Carolina University) for assistance with astrocyte morphological analysis.

CONFLICT OF INTEREST

None declared.

APPENDIX A. SUPPLEMENTARY DATA

Supplementary data to this article can be found online at https://doi.org/10.1016/j.molmet.2020.101136.

REFERENCES

[1] Kuro-o, M., Nabeshima, Y., Matsumura, Y., Aizawa, H., Kawaguchi, H., Suga, T., et al., 1997. Mutation of the mouse klotho gene leads to a syndrome resembling ageing. Nature 390:45—51. https://doi.org/10.1038/36285.

[2] Kurosu, H., Yamamoto, M., Clark, J.D., V Pastor, J., Nandi, A., Gurnani, P., et al., 2005. Suppression of aging in mice by the hormone klotho. Science 309:1829—1833. https://doi.org/10.1126/science.1112766.

[3] Lin, Y., Sun, Z., 2012. Antiaging gene Klotho enhances glucose-induced insulin secretion by up-regulating plasma membrane levels of TRPV2 in MIN6 β-cells. Endocrinology 153:3029—3039. https://doi.org/10.1210/en.2012-1091.

[4] Lin, Y., Sun, Z., 2015. In vivo pancreatic β-cell-specific expression of antiaging gene Klotho: a novel approach for preserving β-cells in type 2 diabetes. Diabetes 64:1444—1458. https://doi.org/10.2337/db14-0632.

[5] Lin, Y., Sun, Z., 2015. Antiaging gene klotho attenuates pancreatic β-cell apoptosis in type 1 diabetes. Diabetes 64:4298–4311. https://doi.org/10.2337/db15-0066.

[6] Rao, Z., Landry, T., Li, P., Bunner, W., Laing, B.T., Yuan, Y., et al., 2019. Administration of alpha klotho reduces liver and adipose lipid accumulation in obese mice. Heliyon 5:e01494. https://doi.org/10.1016/j.heliyon.2019.e01494.

[7] Devaraj, S., Syed, B., Chien, A., Jialal, I., 2012. Validation of an immunoassay for soluble klotho protein. American Journal of Clinical Pathology 137:479–485. https://doi.org/10.1309/AJCPGPMAF7SFRBO4.

[8] Nie, F., Wu, D., Du, H., Yang, X., Yang, M., Pang, X., et al., 2017. Serum klotho protein levels and their correlations with the progression of type 2 diabetes mellitus. Journal of Diabetic Complications 31:594–598. https://doi.org/10.1016/J.JDIACOMP.2016.11.008.

[9] Prud'homme, G.J., Glinka, Y., Kurt, M., Liu, W., Wang, Q., 2020. Systemic Klotho therapy protects against insulitis and enhances beta-cell mass in NOD mice. Biochemical and Biophysical Research Communications. https://doi.org/10.1016/j.bbrc.2020.02.123.

[10] Kim, H.J., Lee, J., Chae, D.W., Lee, K.B., Sung, S.A., Yoo, T.H., et al., 2019. Serum klotho is inversely associated with metabolic syndrome in chronic kidney disease: results from the KNOW-CKD study. BMC Nephrology 20:119. https://doi.org/10.1186/s12882-019-1297-y.

[11] Ji, B., Wei, H., Ding, Y., Liang, H., Yao, L., Wang, H., et al., 2020. Protective potential of klotho protein on diabetic retinopathy: evidence from clinical and *in vitro* studies. J. Diabetes Investig. 11:162–169. https://doi.org/10.1111/jdi.13100.

[12] Hu, M.C., Shi, M., Zhang, J., Addo, T., Cho, H.J., Barker, S.L., et al., 2016. Renal production, uptake, and handling of circulating αklotho. Journal of the American Society of Nephrology 27:79–90. https://doi.org/10.1681/ASN.2014101030.

[13] Leon, J., Moreno, A.J., Garay, B.I., Chalkley, R.J., Burlingame, A.L., Wang, D., et al., 2017. Peripheral elevation of a klotho fragment enhances brain function and resilience in young, aging, and α-synuclein transgenic mice. Cell Reports 20:1360–1371. https://doi.org/10.1016/j.celrep.2017.07.024.

[14] Olauson, H., Mencke, R., Hillebrands, J.-L., Larsson, T.E., 2017. Tissue expression and source of circulating αKlotho. Bone 100:19–35. https://doi.org/10.1016/j.bone.2017.03.043.

[15] Landry, T., Laing, B.T., Li, P., Bunner, W., Rao, Z., Prete, A., et al., 2020. Central α-klotho suppresses NPY/AgRP neuron activity and regulates metabolism in mice. Diabetes 69:db190941. https://doi.org/10.2337/db19-0941.

[16] Nakajima, K., Cui, Z., Li, C., Meister, J., Cui, Y., Fu, O., et al., 2016. Gs-coupled GPCR signalling in AgRP neurons triggers sustained increase in food intake. Nature Communications 7:10268. https://doi.org/10.1038/ncomms10268.

[17] Könner, A.C., Janoschek, R., Plum, L., Jordan, S.D., Rother, E., Ma, X., et al., 2007. Insulin action in AgRP-expressing neurons is required for suppression of hepatic glucose production. Cell Metabolism 5:438–449. https://doi.org/10.1016/j.cmet.2007.05.004.

[18] Wang, Q., Liu, C., Uchida, A., Chuang, J.-C., Walker, A., Liu, T., et al., 2014. Arcuate AgRP neurons mediate orexigenic and glucoregulatory actions of ghrelin. Mol. Metab. 3:64–72. https://doi.org/10.1016/j.molmet.2013.10.001.

[19] Krashes, M.J., Shah, B.P., Madara, J.C., Olson, D.P., Strochlic, D.E., Garfield, A.S., et al., 2014. An excitatory paraventricular nucleus to AgRP neuron circuit that drives hunger. Nature 507:238–242. https://doi.org/10.1038/nature12956.

[20] Chen, G., Liu, Y., Goetz, R., Fu, L., Jayaraman, S., Hu, M.-C., et al., 2018. α-Klotho is a non-enzymatic molecular scaffold for FGF23 hormone signalling. Nature 553:461–466. https://doi.org/10.1038/nature25451.

[21] Zhang, X., Van Den Pol, A.N., 2016. Hypothalamic arcuate nucleus tyrosine hydroxylase neurons play orexigenic role in energy homeostasis. Nature Neuroscience 19:1341–1347. https://doi.org/10.1038/nn.4372.

[22] Varela, L., Horvath, T.L., 2012. Leptin and insulin pathways in POMC and AgRP neurons that modulate energy balance and glucose homeostasis. EMBO Reports 13:1079–1086. https://doi.org/10.1038/embor.2012.174.

[23] Wang, D., He, X., Zhao, Z., Feng, Q., Lin, R., Sun, Y., et al., 2015. Whole-brain mapping of the direct inputs and axonal projections of POMC and AgRP neurons. Frontiers in Neuroanatomy 9:40. https://doi.org/10.3389/fnana.2015.00040.

[24] Zhan, C., Zhou, J., Feng, Q., Zhang, J. -e., Lin, S., Bao, J., et al., 2013. Acute and long-term suppression of feeding behavior by POMC neurons in the brainstem and hypothalamus, respectively. Journal of Neuroscience 33:3624–3632. https://doi.org/10.1523/JNEUROSCI.2742-12.2013.

[25] Al-Qassab, H., Smith, M.A., Irvine, E.E., Guillermet-Guibert, J., Claret, M., Choudhury, A.I., et al., 2009. Dominant role of the p110β isoform of PI3K over p110α in energy homeostasis regulation by POMC and AgRP neurons. Cell Metabolism 10:343–354. https://doi.org/10.1016/J.CMET.2009.09.008.

[26] García-Cáceres, C., Balland, E., Prevot, V., Luquet, S., Woods, S.C., Koch, M., et al., 2019. Role of astrocytes, microglia, and tanycytes in brain control of systemic metabolism. Nature Neuroscience 22:7–14. https://doi.org/10.1038/s41593-018-0286-y.

[27] Yasumoto, Y., Miyazaki, H., Ogata, M., Kagawa, Y., Yamamoto, Y., Islam, A., et al., 2018. Glial fatty acid-binding protein 7 (FABP7) regulates neuronal leptin sensitivity in the hypothalamic arcuate nucleus. Molecular Neurobiology 55:9016–9028. https://doi.org/10.1007/s12035-018-1033-9.

[28] Balland, E., Dam, J., Langlet, F., Caron, E., Steculorum, S., Messina, A., et al., 2014. Hypothalamic tanycytes are an ERK-gated conduit for leptin into the brain. Cell Metabolism 19:293–301. https://doi.org/10.1016/j.cmet.2013.12.015.

[29] Brown, J.M., Scarlett, J.M., Matsen, M.E., Nguyen, H.T., Secher, A., Jorgensen, R., et al., 2019. The hypothalamic arcuate nucleus-median eminence is a target for sustained diabetes remission induced by fibroblast growth factor 1. Diabetes 68:db190025. https://doi.org/10.2337/DB19-0025.

[30] Robins, S.C., Stewart, I., McNay, D.E., Taylor, V., Giachino, C., Goetz, M., et al., 2013. α-Tanycytes of the adult hypothalamic third ventricle include distinct populations of FGF-responsive neural progenitors. Nature Communications 4:1–13. https://doi.org/10.1038/ncomms3049.

[31] Morton, G.J., Matsen, M.E., Bracy, D.P., Meek, T.H., Nguyen, H.T., Stefanovski, D., et al., 2013. FGF19 action in the brain induces insulin-independent glucose lowering. Journal of Clinical Investigation 123:4799–4808. https://doi.org/10.1172/JCI70710.

[32] Rahmouni, K., Haynes, W.G., Morgan, D.A., Mark, A.L., 2003. Intracellular mechanisms involved in leptin regulation of sympathetic outflow. Hypertension 41:763–767. https://doi.org/10.1161/01.HYP.0000048342.54392.40.

[33] Laing, B.T., Huang, H., 2016. Exercise improves hypothalamic function induced by high-fat diet. Immunoendocrinology 3. https://doi.org/10.14800/ie.1446.

[34] Jiang, Z., Rajamanickam, S., Justice, N.J., 2018. Local corticotropin-releasing factor signaling in the hypothalamic paraventricular nucleus. Journal of Neuroscience 38:1874–1890. https://doi.org/10.1523/JNEUROSCI.1492-17.2017.

[35] Zhu, C., Jiang, Z., Xu, Y., Cai, Z.L., Jiang, Q., Xu, Y., et al., 2020. Profound and redundant functions of arcuate neurons in obesity development. Nat. Metab., 1–12. https://doi.org/10.1038/s42255-020-0229-2.

[36] Shi, Y.C., Lau, J., Lin, Z., Zhang, H., Zhai, L., Sperk, G., et al., 2013. Arcuate NPY controls sympathetic output and BAT function via a relay of tyrosine hydroxylase neurons in the PVN. Cell Metabolism 17:236–248. https://doi.org/10.1016/j.cmet.2013.01.006.

[37] Lam, B.Y.H., Cimino, I., Polex-Wolf, J., Nicole Kohnke, S., Rimmington, D., Iyemere, V., et al., 2017. Heterogeneity of hypothalamic pro-opiomelanocortin-expressing neurons revealed by single-cell RNA sequencing. Mol. Metab. 6:383–392. https://doi.org/10.1016/j.molmet.2017.02.007.

[38] Kurosu, H., Ogawa, Y., Miyoshi, M., Yamamoto, M., Nandi, A., Rosenblatt, K.P., et al., 2006. Regulation of fibroblast growth factor-23 signaling by klotho. Journal of Biological Chemistry 281:6120–6123. https://doi.org/10.1074/jbc.C500457200.

[39] Mazucanti, C.H., Kawamoto, E.M., Mattson, M.P., Scavone, C., Camandola, S., 2019. Activity-dependent neuronal Klotho enhances astrocytic aerobic glycolysis. Journal of Cerebral Blood Flow and Metabolism 39:1544–1556. https://doi.org/10.1177/0271678X18762700.

[40] Kunert, S.K., Hartmann, H., Haffner, D., Leifheit-Nestler, M., 2017. Klotho and fibroblast growth factor 23 in cerebrospinal fluid in children. Journal of Bone and Mineral Metabolism 35:215–226. https://doi.org/10.1007/s00774-016-0746-y.

[41] Semba, R.D., Moghekar, A.R., Hu, J., Sun, K., Turner, R., Ferrucci, L., et al., 2014. Klotho in the cerebrospinal fluid of adults with and without Alzheimer's disease. Neuroscience Letters 558:37–40. https://doi.org/10.1016/j.neulet.2013.10.058.

[42] Emami Aleagha, M.S., Siroos, B., Ahmadi, M., Balood, M., Palangi, A., Haghighi, A.N., et al., 2015. Decreased concentration of Klotho in the cerebrospinal fluid of patients with relapsing-remitting multiple sclerosis. Journal of Neuroimmunology 281:5–8. https://doi.org/10.1016/j.jneuroim.2015.02.004.

[43] Hussain, A., Ali, I., Kaleem, W.A., Yasmeen, F., 2019. Correlation between body mass index and lipid profile in patients with type 2 diabetes attending a tertiary care hospital in Peshawar. Pakistan J. Med. Sci. 35:591–597. https://doi.org/10.12669/pjms.35.3.7.

[44] Y.-N. Kim, S. Kim, Y.-O. Cho, Body mass index was positively correlated with blood triglyceride and total cholesterol levels, The FASEB Journal. 26 (2012) lb356–lb356. doi:10.1096/FASEBJ.26.1_SUPPLEMENT.LB356.

[45] Bakari, A.G., Onyemelukwe, C., Sani, B.G., Aliyu, S., Hassan, S.S., Aliyu, T.M., 2007. Relationship between casual blood sugar and body mass index in a suburban northern Nigerian population: a short communication. Nigerian Journal of Medicine 16:77–78. https://doi.org/10.4314/njm.v16i1.37287.

[46] Huo, L., Gamber, K., Greeley, S., Silva, J., Huntoon, N., Leng, X.H., et al., 2009. Leptin-dependent control of glucose balance and locomotor activity by POMC neurons. Cell Metabolism 9:537–547. https://doi.org/10.1016/j.cmet.2009.05.003.

[47] Hentges, S.T., Otero-Corchon, V., Pennock, R.L., King, C.M., Low, M.J., 2009. Proopiomelanocortin expression in both GABA and glutamate neurons. Journal of Neuroscience 29:13684–13690. https://doi.org/10.1523/JNEUROSCI.3770-09.2009.

[48] Rau, A.R., Hentges, S.T., 2017. The relevance of AgRP neuron-derived GABA inputs to POMC neurons differs for spontaneous and evoked release. Journal of Neuroscience 37:7362–7372. https://doi.org/10.1523/JNEUROSCI.0647-17.2017.

[49] Tong, Q., Ye, C.-P., Jones, J.E., Elmquist, J.K., Lowell, B.B., 2008. Synaptic release of GABA by AgRP neurons is required for normal regulation of energy balance. Nature Neuroscience 11:998–1000. https://doi.org/10.1038/nn.2167.

[50] Atasoy, D., Nicholas Betley, J., Su, H.H., Sternson, S.M., 2012. Deconstruction of a neural circuit for hunger. Nature 488:172–177. https://doi.org/10.1038/nature11270.

[51] Marcelin, G., Jo, Y.-H., Li, X., Schwartz, G.J., Zhang, Y., Dun, N.J., et al., 2014. Central action of FGF19 reduces hypothalamic AGRP/NPY neuron activity and improves glucose metabolism. Mol. Metab. 3:19–28. https://doi.org/10.1016/j.molmet.2013.10.002.

[52] Szczypka, M.S., Mandel, R.J., Donahue, B.A., Snyder, R.O., Leff, S.E., Palmiter, R.D., 1999. Viral gene delivery selectively restores feeding and prevents lethality of dopamine-deficient mice. Neuron 22:167–178. https://doi.org/10.1016/S0896-6273(00)80688-1.

[53] Daubner, S.C., Le, T., Wang, S., 2011. Tyrosine hydroxylase and regulation of dopamine synthesis. Archives of Biochemistry and Biophysics 508:1–12. https://doi.org/10.1016/j.abb.2010.12.017.

[54] Satoh, N., Ogawa, Y., Katsuura, G., Numata, Y., Tsuji, T., Hayase, M., et al., 1999. Sympathetic activation of leptin via the ventromedial hypothalamus: leptin-induced increase in catecholamine secretion. Diabetes 48:1787–1793. https://doi.org/10.2337/diabetes.48.9.1787.

[55] Wang, Q., Zhang, M., Ning, G., Gu, W., Su, T., Xu, M., et al., 2011. Brown adipose tissue in humans is activated by elevated plasma catecholamines levels and is inversely related to central obesity. PloS One 6:e21006. https://doi.org/10.1371/journal.pone.0021006.

[56] Laszczyk, A.M., Fox-Quick, S., Vo, H.T., Nettles, D., Pugh, P.C., Overstreet-Wadiche, L., et al., 2017. Klotho regulates postnatal neurogenesis and protects against age-related spatial memory loss. Neurobiology of Aging 59:41–54. https://doi.org/10.1016/j.neurobiolaging.2017.07.008.

[57] D.A. Sarruf, J.P. Thaler, G.J. Morton, J. German, J.D. Fischer, K. Ogimoto, et al, Fibroblast growth factor 21 action in the brain increases energy expenditure and insulin sensitivity in obese rats, (n.d.). doi:10.2337/db09-1878.

[58] Rojas, J.M., Matsen, M.E., Mundinger, T.O., Morton, G.J., Stefanovski, D., Bergman, R.N., et al., 2015. Glucose intolerance induced by blockade of central FGF receptors is linked to an acute stress response. Mol. Metab. 4:561–568. https://doi.org/10.1016/J.MOLMET.2015.05.005.

[59] Jeong, J.H., Lee, D.K., Liu, S.M., Chua, S.C., Schwartz, G.J., Jo, Y.H., 2018. Activation of temperature-sensitive TRPV1-like receptors in ARC POMC neurons reduces food intake. PLoS Biology 16. https://doi.org/10.1371/journal.pbio.2004399.

[60] Chang, Q., Hoefs, S., van der Kemp, A.W., Topala, C.N., Bindels, R.J., Hoenderop, J.G., 2005. The ß-glucuronidase klotho hydrolyzes and activates the TRPV5 channel. Science(80-):310.

